Preclinical Efficacy of BCMA-Directed CAR T Cells Incorporating a Novel D Domain Antigen Recognition Domain

Janine M. Buonato, Justin P. Edwards, Liubov Zaritskaya, Alexandra R. Witter, Ankit Gupta, David W. LaFleur, David A. Tice, Laura K. Richman, and David M. Hilbert

ABSTRACT

Chimeric antigen receptor (CAR) T-cell therapies directed against B-cell maturation antigen (BCMA) have shown compelling clinical activity and manageable safety in subjects with relapsed and refractory multiple myeloma (RRMM). Prior reported CAR T cells have mostly used antibody fragments such as humanized or murine single-chain variable fragments or camelid heavy-chain antibody fragments as the antigen recognition motif. Herein, we describe the generation and preclinical evaluation of ddBCMA CAR, which uses a novel BCMA binding domain discovered from our D domain phage display libraries and incorporates a 4-1BB costimulatory motif and CD3-zeta T-cell activation domain. Preclinical *in vitro* studies of ddBCMA CAR T cells cocultured with BCMA-positive cell lines showed highly potent, dose-dependent measures of cytotoxicity, cytokine production, T-cell degranulation, and T-cell proliferation. In each assay, ddBCMA CAR performed as well as the BCMA-directed scFv-based C11D5.3 CAR. Furthermore, ddBCMA CAR T cells demonstrated *in vivo* tumor suppression in three disseminated BCMA-expressing tumor models in NSG-immunocompromised mice. On the basis of these promising preclinical data, CART-ddBCMA is being studied in a first-in-human phase I clinical study to assess the safety, pharmacokinetics, immunogenicity, efficacy, and duration of effect for patients with RRMM (NCT04155749).

Introduction

Chimeric antigen receptor (CAR) T-cell therapy represents a breakthrough in personalized treatment for relapsed/refractory B-cell malignancies (1, 2). This therapeutic modality has resulted in dramatic clinical responses with high rates of complete remission in patients who have failed multiple prior lines of therapy (3). The success of CD19-targeting CAR T cells has led the FDA to approve four cell therapies for the treatment of B-cell malignancies, including diffuse large B-cell lymphoma, acute lymphoblastic leukemia, follicular lymphoma, mantle cell lymphoma, and primary mediastinal B-cell lymphoma (4–6).

More recently, CAR T-cell therapies have emerged targeting B-cell maturation antigen (BCMA), a cell surface cytokine receptor expressed on some mature B-cell populations, normal plasma cells, and multiple myeloma (7–9). Several BCMA-directed CAR T-cell therapies have shown high overall response rates (ORRs) among patients with relapsed/refractory multiple myeloma (RRMM) who have failed at least three prior therapies, including monoclonal antibodies, second-generation proteasome inhibitors, and immunomodulatory drugs (10–14). The FDA recently approved two BCMA-targeting CAR therapies, idecabtagene vicleucel and ciltacabtagene autoleucel, for the treatment of RRMM.

All approved CAR T-cell therapies and most in development use the prototypic CAR encoding an extracellular antibody-derived antigen-binding domain fused to the intracellular T-cell signaling domain of CD3ζ and a costimulatory domain from CD28 or 4–1BB (15). Although the most-used antigen-binding domains are single-chain variable fragments (scFvs), these domains can aggregate and mispair causing antigen-independent tonic signaling that in turn can result in an exhausted T-cell phenotype and compromised CAR-T function (16–18).

To circumvent some of the inherent structural and functional challenges of scFvs, several alternative binding scaffolds such as ankyrin repeats (19), adnectins (20), thermo-stable DNA-binding proteins (21), and affibodies (22) have been incorporated into CAR constructs. Although some of these domains have been successfully used in the clinic for a variety of applications (23), the clinical utility of alternative scaffolds in CAR T-cell therapy warrants further examination.

Previously, we described the development, characterization, and utilization of D domains as an antigen-binding scaffold in the context of CD123-targeting CAR T cells (24). D domains are small (∼8 kDa) proteins, originally derived from a *de novo*–designed single-domain protein that lacks disulfide bonds (**Fig. 1A**; ref. 25). Herein, we describe the preclinical characterization of CAR T cells incorporating a D domain engineered to specifically engage BCMA and direct the killing of BCMA-expressing multiple myeloma cells. The preclinical data described herein provide continuing support for testing of the clinically manufactured version of this product, CART-ddBCMA in patients with RRMM (NCT04155749).

Materials and Methods

Surface plasmon resonance

Surface plasmon resonance experiments were performed using a Biacore X100 (GE Healthcare). For binding kinetics, measurement of

Arcellx, Inc., Gaithersburg, Maryland.

Note: Supplementary data for this article are available at Molecular Cancer Therapeutics Online (http://mct.aacrjournals.org/).

Corresponding Author: Janine M. Buonato, Arcellx, Inc., 25 West Watkins Mill Road, Suite A, Gaithersburg, MD 20878. Phone: 240-327-0627; E-mail: jbuonato@arcellx.com

Mol Cancer Ther 2022;21:1171–83

doi: 10.1158/1535-7163.MCT-21-0552

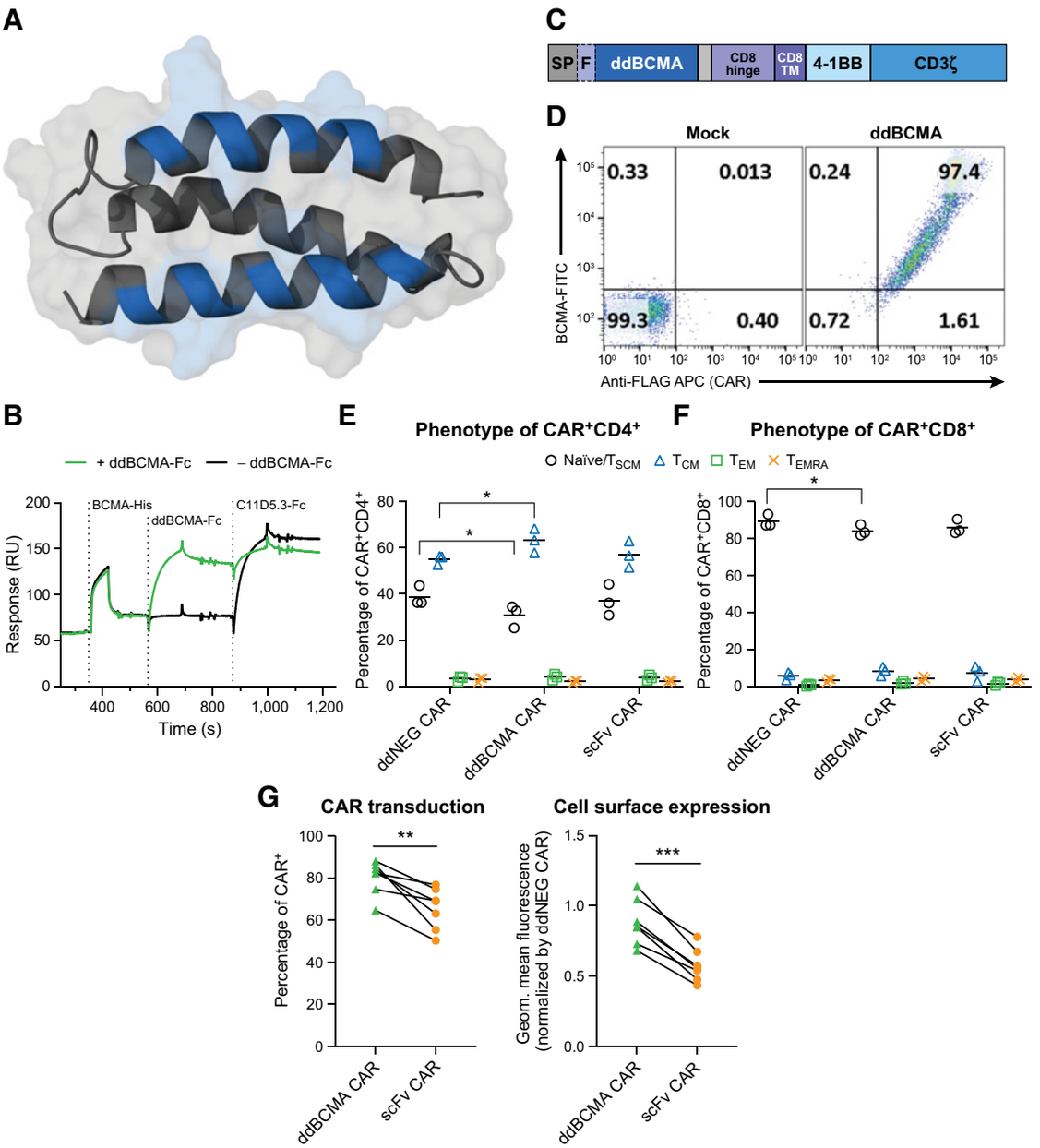

Figure 1.

Design and origin of ddBCMA CAR, a D domain–based chimeric antigen receptor. **A,** A structural model of α3D (PDB 2A3, ref. 25) with the 12 randomized positions of the D domain library highlighted in blue. **B,** To determine whether the epitope for ddBCMA overlaps with C11D5.3 scFv on BCMA, 10 nmol/L BCMA-His was captured on the NTA Chip followed by 100 nmol/L (green) or 0 nmol/L (black) of ddBMCA-Fc injection for 120 seconds, and then followed by a 120-second injection of 100 nmol/L C11D5.3 scFv-Fc. **C,** Map of ddBCMA CAR expression cassette cloned into a lentiviral transfer plasmid (SP, signal peptide; F, flag tag). **D,** Mock or ddBCMA CAR–transduced T cells were analyzed by flow cytometry for CAR expression (using APC-conjugated anti-FLAG antibody) and binding to FITC-labeled BCMA protein. **E** and **F,** Phenotyping is shown for three individual donor T-cell lots transduced with ddNEG CAR, ddBCMA CAR, or scFv CAR. Cells were stained for CD4, CD8, CD62L, and CD45RA. Naïve or stem cell memory (Naïve/T_{SCM}; $CD62L^+/CD45RA^+$), central memory (T_{CM}, $CD62L^+/CD45RA^-$), effector memory (T_{EM}; $CD62L^-/CD45RA^-$), and T_{EMRA} ($CD62L^-/CD45RA^+$) populations were quantified for the $CD4^+$ (**E**) and $CD8^+$ (**F**) populations. **G,** Cell surface expression (percentage of CAR) and geometric mean fluorescence of CAR^+ cells normalized to ddNEG CAR expression are shown for paired samples of ddBCMA CAR and scFv CAR from 7 independent T-cell lots; ***, $P < 0.001$; **, $P < 0.01$; *, $P < 0.05$ by paired one-way ANOVA (**E** and **F**) or paired *t*-test (**G**).

ddBCMA, 122 RU of BCMA-Fc expressed in HEK293F cells and purified using Protein A chromatography was immobilized on a research-grade sensor CM5 Chip (GE Healthcare) by amine coupling. The experiment was performed in HBS-EP^+ pH 7.4 (GE Healthcare) as the binding buffer at 25°C. Purified ddBCMA with a C-terminal HIS tag was transiently expressed in HEK293F cells and injected over the flow cell at concentrations of 100, 33.3, 11.1, 3.7, and 1.23 nmol/L at a flow rate of 30 μL/min. ddBCMA binding was measured during

the association and dissociation times of 120 and 600 seconds, respectively. The surfaces were regenerated between cycles with a 120-second injection of 10 mmol/L Glycine pH 2.0. The injections were done in a random order for the various concentrations. The data were fit to a simple 1:1 interaction model using the local Rmax fitting data analysis option available within Biacore X100 Evaluation software.

Generation of CAR constructs

Double-stranded DNAs encoding ddBCMA, ddNEG (negative control α3D; ref. 25), and C11D5.3 scFv (26–28) were synthesized as gBlocks (Integrated DNA Technologies) and restriction digest cloned into a lentiviral construct—pELNS—encoding a CAR with the following components in order: Chymotrypsinogen signal peptide, FLAG tag, 2×G_4S linker, antigen-binding domain, 2×G_4S linker, CD8 hinge and transmembrane domains, 4-1BB and CD3ζ intracellular signaling domain.

In some experiments, including the MM.1S mouse xenograft study, an alternative lentiviral plasmid, pSMPUW (Cell BioLabs), was used into which the ddBCMA CAR and ddNEG CAR lacking FLAG tag were cloned.

Lentivirus production and transduction

Lentivirus was produced from 293T cells using three packaging plasmids (pMD2.G, pRSV-REV, and pMDLg/pRRE) and the appropriate transfer vector plasmid, as previously described (24). In certain experiments, the transfer vector was pLentiCRISPRv2, which contained a guide sequence specifically designed to disrupt the human BCMA gene.

Primary human T cells negatively selected from cryopreserved human peripheral blood mononuclear cells using the Miltenyi Pan T-cell isolation kit (Miltenyi Biotec) were activated and transduced as described previously (24). Cells were generally used between days 7 and 11 after activation for *in vitro* experiments and assayed for expression of the CAR on day 6 or 7. Information on T-cell lots used throughout, including the percentages of CAR^+ and staining GMF, is given in Supplementary Table S1.

Cell lines engineered for CRISPR-mediated BCMA knockout were transduced following a similar procedure.

Cell lines

Cell lines RPMI8226 (ATCC cat. No. CRM-CCL-155, RRID: CVCL_0014), NCI-H929 (ATCC cat. No. CRL-9068, RRID: CVCL_1600), U266 (ATCC cat. No. TIB-196, RRID:CVCL_0566), MM.1S (ATCC cat. No. CRL-2974, RRID:CVCL_8792), IM9 (ATCC cat. No. CCL-159, RRID:CVCL_1305), SKW6.4 (ATCC cat. No. TIB-215, RRID:CVCL_3796), Daudi (ATCC cat. No. CCL-213, RRID: CVCL_0008), and BCMA-negative K562 (ATCC cat. No. CCL-243, RRID:CVCL_0004), were obtained from the ATCC. MOLM13 was a kind gift from Terry Fry (24). Cell lines authenticated by morphology and cell surface phenotyping for BCMA were maintained in culture for a maximum of 20 passages. *Mycoplasma* testing was performed on cell line stocks for any cells used in animal studies.

The bioluminescence imaging vector MSCV.FLuc.EF1a.copGFP.T2A.Puro (System Bioscience) was introduced into NCI-H929, U266, MM.1S, MOLM13, IM9, and Daudi via lentiviral transduction. Transduced cells were selected for integration via puromycin resistance and single-cell cloning of GFP/Luciferase expressing NCI-H929 and U266 cells was performed to select for high luciferase activity.

Lentivirus containing BCMA-specific gRNA sequence (targeting the extracellular domain of BCMA) and Cas9 was transduced into NCI-H929 and RPMI-8226 cells, and selection and single-cell cloning were performed to generate $BCMA^{-/-}$ cell lines.

Signaling assay with Jurkat cells

A reporter cell line for Nuclear Factor of Activated T-cells (NFAT) signaling was generated from Jurkat E6.1 cells (Sigma) transduced with Cignal Lenti NFAT Reporter virus (Qiagen) using SureENTRY Transduction reagent (Qiagen). Transduced cells were selected with puromycin then single cell cloned. A clonal pathway reporter cell line, JNL10, was selected on the basis of its responsiveness to stimulation with plate-bound mouse anti-human CD3 antibody (Clone OKT3, eBioscience, RRID:AB_467057).

To assess CAR signaling activity, JNL10 reporter cells were electroporated with CAR constructs using a Bio-Rad GenePulser and cultured at 37°C overnight in a 12-well plate. The next day, electroporated JNL10 cells were activated with target cells by incubating at approximately 1:1 ratio in 100-μL culture medium in a 96-well plate for 5 hours at 37°C. NFAT-mediated signaling was monitored by the subsequent addition of Luciferase substrate (Bright-Glo, Promega or BriteLite, PerkinElmer) and measuring relative luminescence units using a plate reader. Target cells with and without electroporated JNL10 cells were used as the background control. Percentage of CAR expression on JNL10 cells was measured in parallel by staining with PE-conjugated anti-FLAG antibody (BioLegend, RRID:AB_2563147).

Cytotoxicity assay

Cytotoxicity mediated by BCMA-targeted CAR T cells was measured using luciferase-expressing target cells as a correlate for cytotoxic activity of CAR T cells. T cells were cultured overnight with the indicated cell lines expressing GFP/Luciferase at a range of effector to target (E:T) ratios starting with a 1:2 or 1:4 ratio (20,000 or 10,000 CAR^+ T cells to 40,000 target cells) down to approximately 1:256. After overnight incubation, remaining luciferase activity was assessed using the Synergy2 plate reader (BioTek) and normalized to maximum signal to measure cytotoxic activity. All conditions were run in triplicate in 96-well format.

Cytokine release assay

Cytokine release assays were performed 7 to 14 days after T-cell activation with 25,000 CAR^+ T cells cultured alone or with 25,000 target cells (1:1) overnight in 0.2 mL of AIM-V media in a 96-well U-bottom plate. Equal numbers of CAR^+ cells were used to equalize the number of potentially reactive cells in the culture. All conditions were run in triplicate. In sBCMA experiments, CAR^+ T cells at multiple E:T ratios were cultured overnight with 40,000 target cells in the absence or presence of recombinant BCMA-HIS (ACRO Biosystems). For restimulation experiments, supernatants were harvested from cytotoxicity assay plates and used for cytokine release analysis.

After overnight culture, plates were centrifuged for 5 minutes at 1200 RPM and supernatants were collected. IL2 and IFNγ concentrations were assessed by ELISA using the human IL2 and IFNγ *Ready-SET-Go* uncoated ELISA kits (eBioscience) or Human IL2 or IFNγ DuoSet ELISA kits (R&D Systems) according to the manufacturers' instructions. All supernatants were diluted 5 to 30x in recommended buffer and 100 μL of diluted supernatant was added per well. After concentrations were calculated according to the standard curve, each value was multiplied by the dilution factor.

Antibodies and reagents

A table of antibodies used throughout this study is given in Supplementary Methods.

For the binding experiment in **Fig. 1**, recombinant human BCMA-Fc (R&D Systems) was FITC labeled with a FITC labeling kit (Millipore/Sigma) according to the manufacturer's instructions. A total of 0.1×10^6 CAR T cells were incubated with 0.5 μg of BCMA-FITC at 4°C, and then washed twice before flow cytometry. In sBCMA experiments, triplicate samples of 20,000 CAR T cells were incubated in FACS buffer for 30 minutes at 4°C or in T-cell media for 16 to 18 hours at 37°C with one of the following conditions: $BCMA^+$ target cells (H929-GFP/luc; E:T = 1:2), no stimulation, 0.5 or 1.5 μg/mL sBCMA (BCMA-HIS, Acro Biosystems). At the end of incubation, cells were stained for BCMA binding (4°C incubation) or CD69/4–1BB expression (37°C incubation) and analyzed by flow cytometry.

Degranulation and intracellular cytokine staining

Degranulation assays were performed with transduced T cells on day 8 after activation. In these assays, 5×10^4 CAR^+ T cells were cultured with 1×10^5 target cells (1:2) for 4 hours in 0.2 mL of media in a 96-well U-bottom plate. Cells were cultured in the presence of PE-conjugated CD107a antibody (BioLegend, RRID: AB_1186062) and monensin (included to prevent degradation of endocytosed anti-CD107a antibody; BioLegend). After 5 hours of culture, cells were washed twice then fixed and permeabilized and using the Cytofix/Cytoperm kit (BD Biosciences) for 20 minutes at 4°C. Cells were then washed in permeabilization buffer and stained with APC-conjugated anti-Human IFNγ (BioLegend) and FITC anti-CD3 (BioLegend).

Proliferation assay

Transduced T cells 9 to 11 days after activation were washed and cultured overnight in IL2-free media to return the cells to a more quiescent state. The following day, cells were washed in dPBS and labeled with BD Horizon Violet Proliferation Dye 450 (VPD450, BD Biosciences). CAR^+ T cells (25,000) were cultured alone or with target cells (1:1) for 96 hours in 0.2 mL of complete media in a 96-well U-bottom plate. After 96 hours, plates were centrifuged and cells were stained with APC anti-Human CD3 (BioLegend). Cells were then washed twice, resuspended, and run via flow cytometry using a high-throughput sampler collecting total events in 150 of 200-μL cell suspension. Total $CD3^+$ cells were then enumerated to assess cell proliferation, which was also evidenced by the dilution of VPD450 in daughter cells. All conditions were run in triplicate.

T-cell restimulation assay

A restimulation experiment was set up with ddNEG, ddBCMA, and scFv CAR T cells each with three separate flasks that were cultured in parallel and maintained throughout the study. In each flask 0.75×10^6 CAR^+ T cells were combined with 1.5×10^6 H929-GFP/luc cells (E:T = 1:2) in T-cell media at 37°C. After 4 days, CAR^+ T cells were counted to determine expansion at the end of the stimulation round (Stim 1). Subsequent rounds of stimulation (Stim 2–4) were initiated with 0.75×10^6 CAR^+ T cells from the previous round combined with H929 target cells (E:T = 1:2) in fresh media. In addition, to assess functional capacity of post-stimulation cells from each round, CAR^+ T cells were used in cytotoxicity and cytokine release experiments as described above. Fold change in number of CAR^+ T cells was determined by normalizing total cell counts by percentage of $CD3^+CAR^+$ cells from flow cytometric analysis then calculating fold change based on setup (0.75×10^6 CAR T cells).

Mouse studies

All studies took place at Noble Life Sciences and were approved by their IACUC (approval NLS-420).

Either 5×10^6 U266-GFP/LUC (BCMA-expressing human myeloma-derived tumor cells) or 2×10^6 MM.1S-GFP/LUC tumor cells were injected into NOD.Cg-*Prkdc*^{scid} *Il2rg*^{tm1Wjl}/SzJ (NSG, RRID: IMSR_JAX:005557) mice intravenously via the tail vein. Once disseminated tumor burden was established (37 and 23 days after tumor cell injection for U266 and MM.1S, respectively), mice were injected intravenously with the indicated CAR T cells. Cryopreserved CAR T cells were thawed and cultured overnight in complete T-cell media supplemented with IL2 before transfer. Animals were dosed intraperitoneally (3 mg/mouse) with XenoLight D-Luciferin Potassium Salt (PerkinElmer) then imaged 4 minutes later using an *in vivo* imaging system (IVIS Lumina LT Series III, PerkinElmer). Collected images were analyzed using Living Image software (PerkinElmer, RRID: SCR_014247) exclusively using images acquired for 4 minutes. Images were scaled in the radiance setting with a scale of 10^4 to 10^6 radiance units (photons/sec/cm^2/sr) and exported before compilation.

On day 14 after CAR T-cell transfer, 200 to 250 μL of blood was collected into heparinized tubes via the retroorbital route, transferred to 96-well V-bottom plates and centrifuged to pellet cells. Red blood cells were lysed with ACK-lysis buffer three times, and then stained with the indicated antibodies. Samples were resuspended in 175 μL of flow cytometry buffer. One hundred fifty microliters of the sample was collected and analyzed via a High Throughput Sampler and BD Celesta flow cytometer.

Necropsies were performed in the MM.1S tumor study on day 15 after T-cell transfer for mice that received HBSS, ddNEG CAR, and 0.15×10^6 ddBCMA CAR T cells and on day 21 for all other groups, except for one mouse in the 4.5×10^6 ddBCMA CAR T-cell group that was euthanized on day 11 after observation of neurological symptoms (walking in circles). Fixed tissues were paraffin embedded, sectioned, and stained with hematoxylin and eosin.

Statistical analysis

Where indicated, statistical analysis was performed using ordinary one-way or two-way ANOVA with the Tukey's multiple comparison test using GraphPad Prism 8.0 Software (GraphPad Software Inc., RRID:SCR_002798).

Data availability

Data were generated by the authors and included in the article.

Results

ddBCMA CAR Construction

The BCMA-binding D domain was identified through the directed evolution of D domain phage libraries (**Fig. 1A**; ref. 24; selected for binding to human BCMA-Fc), followed by targeted mutagenesis to remove potentially immunogenic epitopes. The resulting 73 amino acid D domain (ddBCMA) has an affinity for human BCMA of K_D = 14 nmol/L ($k_{on} = 4.1 \times 10^6$ $M^{-1}s^{-1}$, $k_{off} = 0.056$ s^{-1}) as measured by surface plasmon resonance and is predicted to have low MHC class II–mediated immunogenicity (Supplementary Table S2). Additional kinetics measurements showed that the epitope for ddBCMA binding to BCMA overlaps with C11D5.3, a murine monoclonal antibody previously reported to be specific for human BCMA (**Fig. 1B**; refs. 7, 26). When the two BCMA-binding domains were each fused to human IgG-Fc, the measured affinities for monovalent BCMA were K_D = 33 nmol/L ($k_{on} = 2.0 \times 10^6$ $M^{-1}s^{-1}$, $k_{off} = 0.065$ s^{-1}) for

ddBCMA and $K_D = 3.3$ nmol/L ($k_{on} = 1.4 \times 10^6\ M^{-1}s^{-1}$, $k_{off} = 4.7 \times 10^{-3}\ s^{-1}$) for C11D5.3, where the most notable difference in binding kinetics is a faster off-rate for ddBCMA.

To further define the specificity of the binding domain, ddBCMA-Fc was used in a human tissue cross-reactivity study using cryopreserved human tissues (Supplementary Methods). Specificity of staining was established during protocol development as described (Supplementary Methods). Specific ddBCMA-Fc binding was observed in sections of splenic red pulp where plasma cells are known to reside (29). Low levels of binding were detected in placenta (Hofbauer and endothelial cells), skin (dermal nerves), testis (Sertoli cells), and uterus (perivascular cells), but it should be noted that such staining was primarily cytoplasmic and only observed at the highest ddBCMA-Fc concentration of 10 μg/mL (Supplementary Table S3). Follow-up on these findings using primary cells or cell lines derived from some of these tissues as well as other major tissues confirmed no nonspecific cytolytic activity of ddBCMA CAR T cells (Supplementary Table S4).

The ddBCMA D domain CAR was assembled and incorporated into a third-generation lentiviral transfer vector as described in Materials and Methods and illustrated in **Fig. 1C**. For comparison, we constructed identical lentiviral constructs replacing ddBCMA with the well-characterized BCMA-binding scFv C11D5.3 (ref. 26; herein referred to as scFv CAR) or a D domain with no known target antigen (ddNEG CAR).

To test the ability of ddBCMA to mediate antigen recognition, normal donor T cells were transduced with ddBCMA CAR lentivirus or mock transduced and incubated with FITC-labeled recombinant BCMA, which showed that nearly all cells (97.4%) expressed CAR and bound BCMA (**Fig. 1D**). In addition, due to the unique scaffold for ddBCMA, we were able to isolate and develop D domain–specific antibodies to be used in FLAG-free detection of the ddBCMA CAR on the surface of T cells (Supplementary Fig. S1).

Normal T cells from three different donors were transduced in parallel with lentiviral vectors encoding ddBCMA CAR, ddNEG CAR, or scFv CAR and stained for CD4, CD8, CD62L, and CD45RA. ddBCMA CAR T cells had very low percentages of effector memory and terminally differentiated T_{EMRA} cells, and $CD8^+$ cells were almost all naïve/stem memory cell phenotypes (**Fig. 1E** and **F**). The overall abundance of $CD4^+$ and $CD8^+$ cells varies with time in culture and from donor to donor. Although the phenotype of transduced T cells did not vary significantly between ddBCMA and scFv CAR, there was a consistent pattern of reduced CAR positivity and cell surface expression levels for scFv CAR compared with ddBCMA CAR (**Fig. 1G**; Supplementary Table S1). In at least a subset of samples, this was also linked to lower CAR integration (Supplementary Fig. S2).

In vitro activation and antitumor activity of ddBCMA CAR T cells

T cells expressing ddBCMA CAR were assessed for their ability to activate antigen-specific intracellular signaling and cytolytic function. T cells expressing a well-characterized BCMA-binding scFv C11D5.3 (scFv CAR), or a CAR with no known target antigen, the α3D-CAR (ddNEG CAR), were used as positive and negative controls, respectively.

As detailed in **Fig. 2A**, a panel of BCMA-expressing tumors induced NFAT-specific signaling in Jurkat cells expressing ddBCMA CAR and a NFAT-RE/luciferase reporter gene. A similar pattern of NFAT activation was also observed in scFv CAR expressing Jurkat reporter cells. The BCMA specificity of this response was confirmed by the inability of the BCMA-negative cell lines K562 and H929 KO (homozygous BCMA CRISPR knockout) to induce NFAT signaling in ddBCMA CAR– or scFv CAR–expressing cells. These results also suggest little to no antigen-independent signaling was mediated by either CAR.

The functional properties of ddBCMA CAR were further assessed in a cytolytic assay in which CAR T cells were cocultured with BCMA positive cell lines (U266, Daudi, IM9, H929) or the BCMA-negative acute myelogenous leukemia cell line, MOLM13. The data in **Fig. 2B** show that ddBCMA and scFv CARs mediated BCMA-specific cytolytic activity across a range of effector to target (E:T) ratios when cocultured with BCMA-positive tumor cells. The panel of cell lines varied in their relative BCMA expression (Supplementary Fig. S3), and the extent of CAR-T–mediated target cell lysis moderately correlated with BCMA cell surface expression. Although there is a less clear correlation between target density and NFAT reporter activity, this may reflect the timepoint used to quantify intracellular signaling that is inherently dynamic in nature.

To assess additional hallmarks of CAR-mediated T-cell activation, IL2 and IFNγ secretion was measured in cocultures of CAR expressing T cells with a panel of tumor cell lines. ddBCMA CAR T cells induced similar levels of IL2 and IFNγ release as scFv CAR T cells in response to culture with the BCMA-expressing target cells, but importantly not the BCMA-negative K562 nor BCMA-knockout RPMI-8226 cells (**Fig. 3A** and **B**). The nonbinding ddNEG CAR produced little or no cytokine following coculture with all target cells, thus demonstrating that the antigen specificity of a D domain determines its biological function and not an inherent structural motif common to all D domains.

Another hallmark of antigen-specific T-cell activation is the release of apoptosis-inducing cytolytic granules in a process referred to as degranulation and the concomitant appearance of the lysosomal protein CD107a/LAMP-1 on the cell surface (30). Accordingly, degranulation of CAR^+ T cells, as measured by CD107a expression was assessed with BCMA-expressing H929 cells or BCMA knockout cells, H929-$BCMA^{-/-}$. In this experiment, the scFv and ddBCMA CAR T cells expressed CD107a and produced intracellular IFNγ when cocultured with the H929 cells, but importantly, not H929-$BCMA^{-/-}$ cells (**Fig. 3C** and **D**). ddNEG CAR T cells failed to upregulate CD107a and IFNγ. The percentage of $CD107a^+$ or $IFN\gamma^+$ T cells was normalized on the basis of the percentage of expression of the corresponding CAR (ddNEG, ddBCMA, and scFv CAR were $86.9\%^+$, $87.6\%^+$, and $74.4\%^+$, respectively, Supplementary Table S1).

Given that ddBCMA CAR-potentiated BCMA-dependent T-cell signaling, target cell lysis, and cytokine release, we next sought to measure whether this activity led to T-cell proliferation, a key requirement for antitumor CAR activity *in vivo*. After a 4-day coculture with target cells, ddBCMA CAR T cells had a strong proliferative response to the BCMA-expressing cell lines RPMI-8226, H929, and U266, but not to BCMA-negative MOLM13 (**Fig. 3E**). The nonbinding ddNEG CAR did not show any significant proliferation.

Previous studies have noted serum levels of soluble BCMA (sBCMA) in patients with multiple myeloma with an average concentration of 0.5 up to approximately 1.5 μg/mL (31). At these significant levels, it is conceivable that sBCMA could interfere with the ability of CAR T cells to engage BCMA-positive myeloma cells. To assess the impact that sBCMA may have on ddBCMA CAR activity, a series of *in vitro* experiments were performed in the presence of added sBCMA. Though sBCMA bound with high efficiency to the CAR T-cell surface (**Fig. 3F**), no physiologically relevant levels of T-cell activation were seen in the absence of BCMA-positive target cells (**Fig. 3G**).

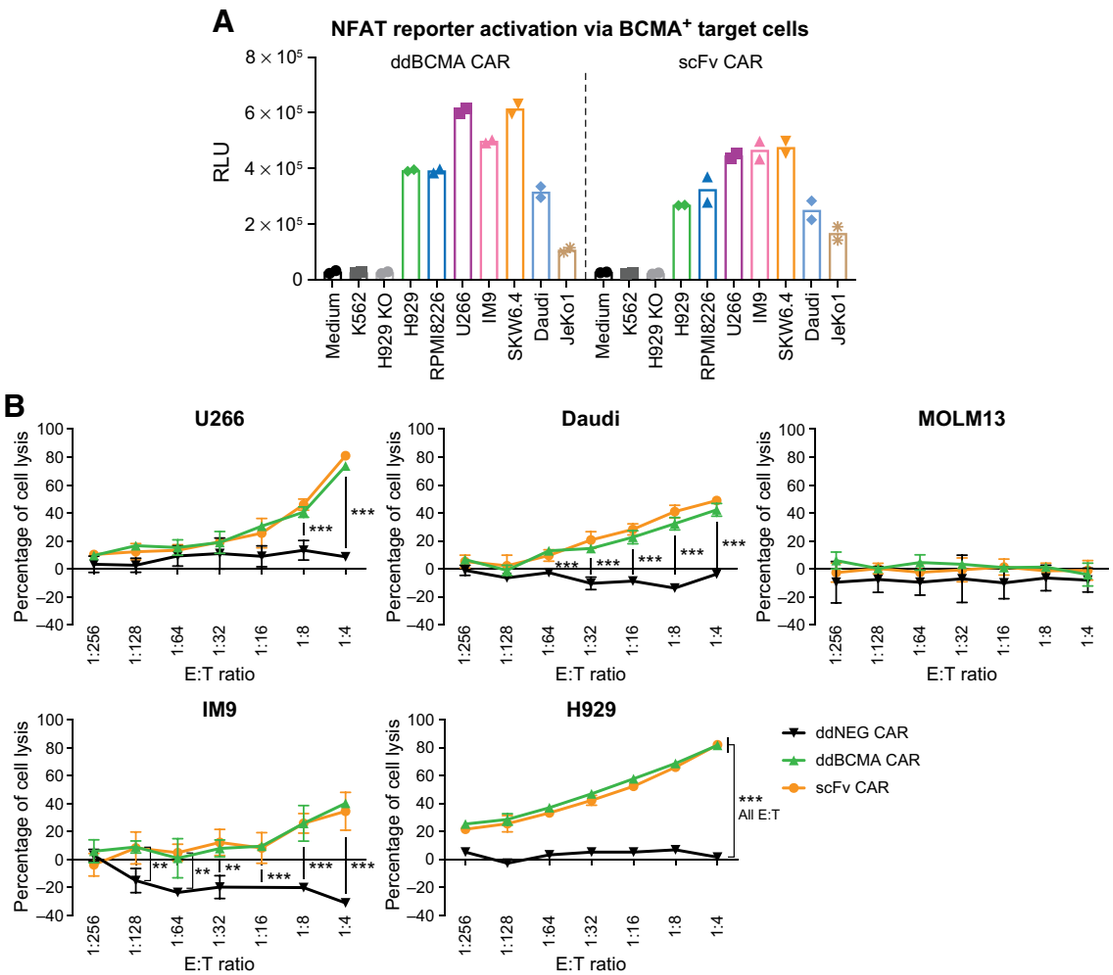

Figure 2.

ddBCMA CAR induces T-cell signaling and lysis of a panel of BCMA-positive tumor cell lines. **A,** Jurkat reporter cells transfected with ddBCMA CAR or scFv CAR were cultured at a 1:1 ratio with the indicated cell lines for 5 hours, followed by luciferase substrate addition and measurement of luciferase activity. Average relative luminescence units (RLUs) signal is shown with individual data points ($n = 2$) from a representative experiment performed a total of four times. **B,** Cell lysis experiments were performed with titrated dilutions of ddNEG, ddBCMA, and scFv CAR transduced T cells cultured with 40,000 cells of the indicated cell lines. Calculated the percentage of lysis is shown as mean ± s.e.m. ($n = 3$). **B,** ***, $P < 0.001$; **, $P < 0.01$ for both ddBCMA CAR and scFv CAR compared with ddNEG CAR by two-way ANOVA.

Across a range of E:T ratios, the addition of 1.5 or 0.5 μg/mL sBCMA to the coculture of ddBCMA CAR T and H929 target cells had no impact on target cell lysis (**Fig. 3H**). Cytokine release remained high with the addition of sBCMA, though it was slightly impaired at some E:T ratios (**Fig. 3I** and **J**).

An additional method of testing the T-cell activity *in vitro* to better approximate *in vivo* efficacy and anticipate T-cell exhaustion is a repeated stimulation long-term expansion culture (32). Upon repeated exposure to H929 target cells in culture, ddBCMA CAR T cells were assessed for proliferation, cytotoxic activity, and capacity for target-induced IL2 secretion (**Fig. 4A–C**). Although proliferative capacity and IL2 release were significantly impaired after round two of stimulation (Stim 2), ddBCMA CAR T cells remained capable of inducing H929 lysis through Stim 4. In agreement with other *in vitro* assessments, ddBCMA CAR T cells performed equivalently to scFv CAR T cells in all measures.

ddBCMA CAR T cells demonstrate *in vivo* antitumor activity

The *in vitro* activities observed with ddBCMA CAR T cells and equivalence to a scFv CAR with known *in vivo* and clinical activity supported further analysis of *in vivo* antitumor activity. Accordingly, NSG mice with established U266 xenografts received a single dose of 1.5×10^6 CAR-positive T cells transduced with ddNEG, ddBCMA, or BCMA scFv CAR. Preinfusion transduced T cells were phenotyped for CD4, CD8, CD45RA, and CD62 L (Supplementary Fig. S4). As seen previously in **Fig. 1E**, CAR^+CD8 T cells from all groups displayed primarily a naïve/T_{SCM} phenotype with a low proportion of terminally differentiated T_{EMRA} cells. CAR^+CD4 T cells were primarily of the naïve/T_{SCM} or T_{CM} phenotype, with a small proportion of T_{EM} phenotype cells (Supplementary Fig. S4). Complete tumor regression was observed for both BCMA-targeted CAR-T products by day 11 and was maintained for 32 days after CAR T-cell administration (**Fig. 4D** and **E**). Similar trends were observed for ddBCMA versus scFv CAR T

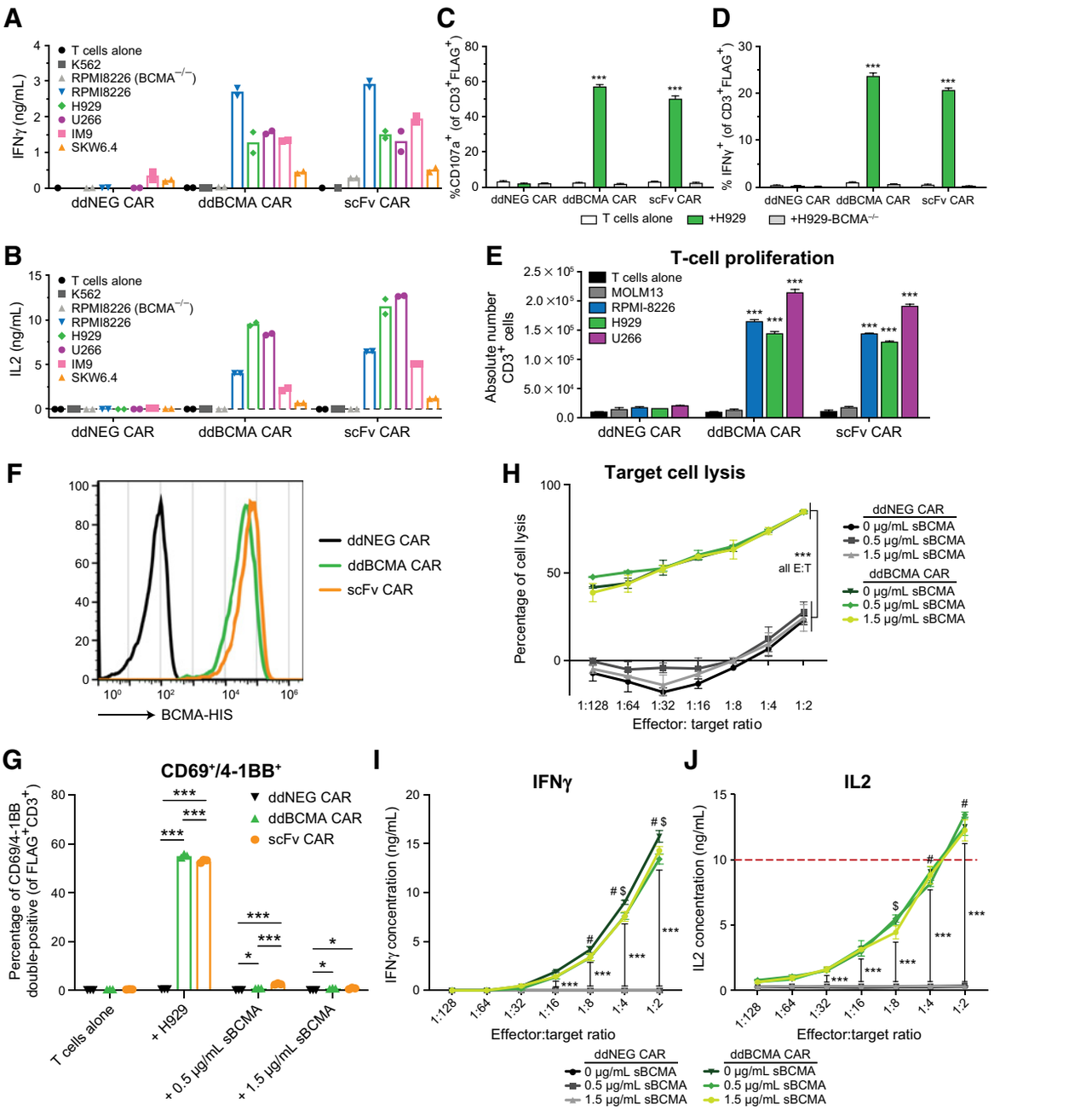

Figure 3.

Measures of T-cell activation from ddBCMA CAR engagement with target cells. **A** and **B,** IFNγ and IL2 cytokines were measured from 16 hours cocultures of ddNEG, ddBCMA, or scFv CAR-transduced T cells and indicated cell lines at 1:1 E:T ratio. Cytokine concentration measurements are shown as mean with individual data points ($n = 2$) from a representative experiment repeated five times with three different donors. **C,** CD107a surface staining and **D**. intracellular IFNγ was measured from T cells after 5 hours of coculture with the indicated cell lines. Percentage of positive staining of the $CD3^+FLAG^+$ population is shown as average ± s.e.m. ($n = 3$) from a representative experiment repeated five times with two different donors. **E,** $CD3^+$ T-cell counts were measured by flow cytometry after 4 days coculture with the indicated cell lines; shown as average ± s.e.m. ($n = 3$) from a representative experiment repeated twice. **F,** Binding of soluble BCMA (sBCMA) to the indicated T cells was assessed via flow cytometry **G**. 4-1BB and CD69 double-positive T cells were quantified by flow cytometry after incubation with H929 target cells or sBCMA, as shown ($n = 3$; representative of two experiments). **H,** Cell lysis experiments were performed with titrated T cells cultured in the presence of 40,000 H929 cells and the indicated concentration of sBCMA. The calculated percent lysis is shown as mean ± s.e.m. ($n = 3$). **I** and **J,** IFNγ and IL2 cytokines were measured from supernatants collected in **H**. Red dotted line indicates upper limit of quantification from standard curve for IL2 ELISA. Data in **H–J** are from a representative experiment repeated with three different donors. **C–E,** ***, $P < 0.001$ for indicated target cells compared with T cells alone or H929 $BCMA^{-/-}$ and compared with ddNEG CAR. **G,** ***, $P < 0.001$; **, $P < 0.01$; *, $P < 0.05$ by two-way ANOVA. **H–J,** ***, $P < 0.001$ comparing all ddBCMA CAR conditions with all ddNEG conditions; #, $P < 0.05$ for 0 versus 0.5 µg/mL sBCMA; $, $P < 0.05$ for 0 versus 1.5 µg/mL sBCMA. All statistics calculated by two-way ANOVA with Tukey's correction for multiple comparisons.

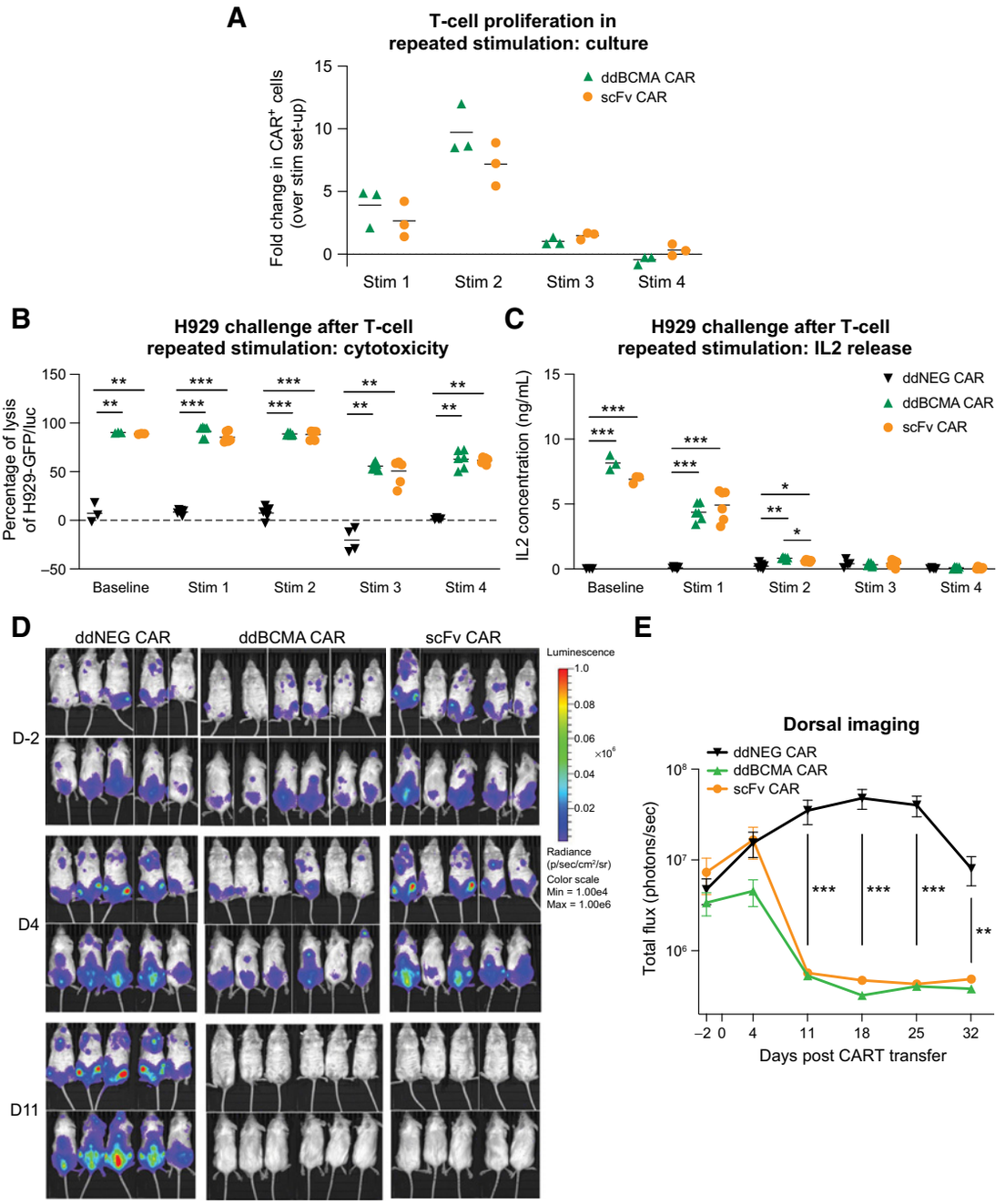

Figure 4.

Long-term *in vitro* expansion and *in vivo* efficacy of ddBCMA CAR T cells. **A–C,** ddNEG, ddBCMA, and scFv CAR T cells were subjected to four rounds of stimulation with H929 GFP/luc cells and assessed throughout for proliferation (**A**), cytotoxic function (**B**), and cytokine production (**C**). Data shown are calculated from triplicate cultures maintained in parallel and are representative of three independent experiments. **D** and **E,** Xenografts were established for 37 days in NSG mice by intravenously injection of 2×10^6 U266 cells, followed by single intravenously infusion of 1.5×10^6 CAR^+ T cells (day 0). Tumor burden, as measured by luminescence signal, was monitored by IVIS imaging as shown in **D** and quantified in **E**. ***, $P < 0.001$; **, $P < 0.01$; *, $P < 0.05$ calculated by one-way ANOVA in **A–C** and two-way ANOVA in **D** and **E** with Tukey's correction for multiple comparisons.

cells using xenografts of the B-cell leukemia cell line NALM6 engineered to express BCMA (Supplementary Fig. S5).

We next sought to further characterize ddBCMA CAR T-cell *in vivo* activity and safety using MM.1S cells, a more aggressive myeloma tumor model. Mice receiving ddBCMA CAR T cells demonstrated a clear dose-dependent clearance of the tumor in which mice receiving 0.5×10^6 ddBCMA CAR T cells displayed minimal antitumor activity whereas mice treated with 4.5×10^6 ddBCMA CAR T cells displayed

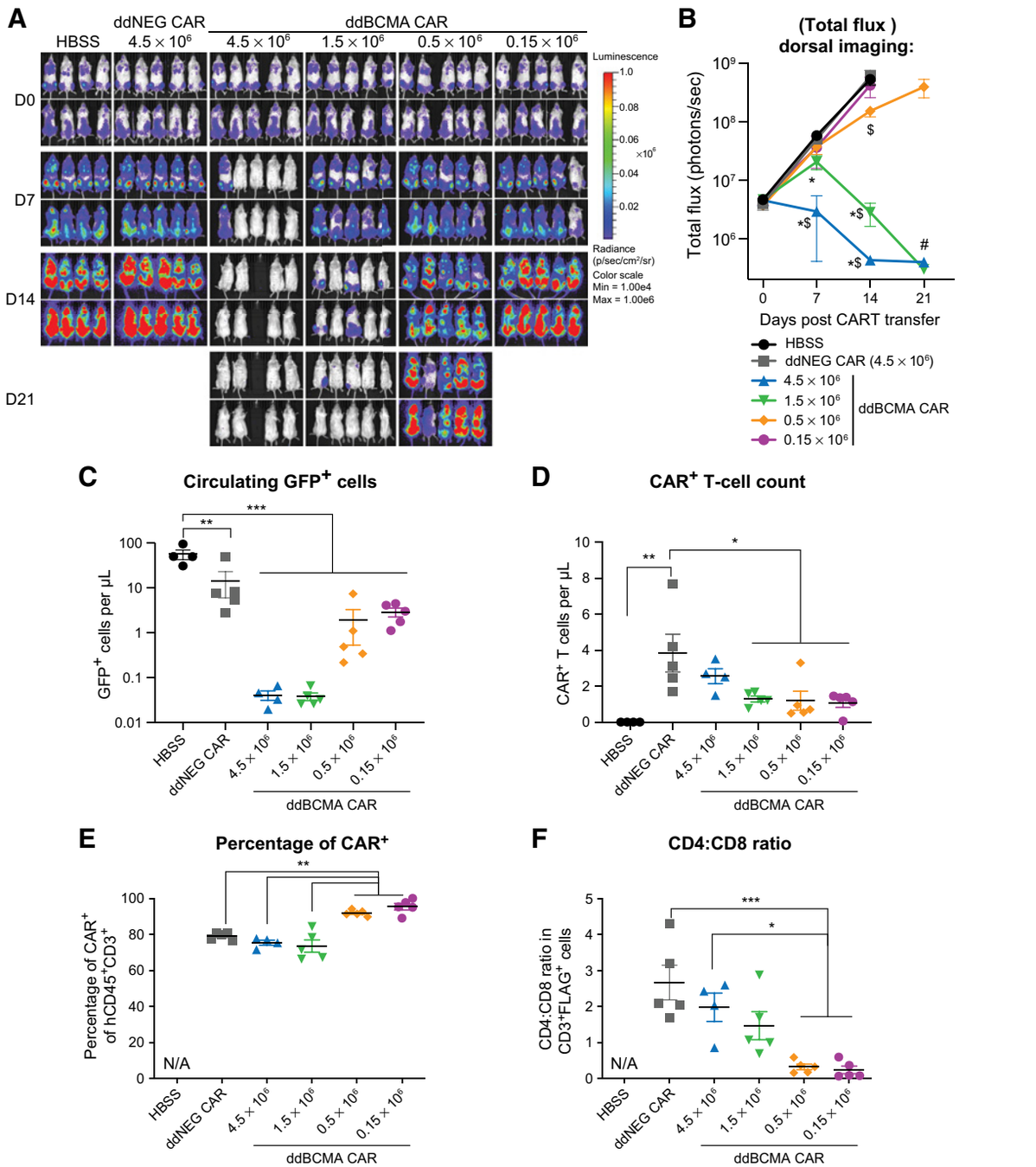

Figure 5.

ddBCMA CAR T-cell *in vivo* activity is dose dependent. Xenografts were established in NSG mice for 23 days following intravenous injection of 2×10^6 MM.1S cells, followed by single intravenous infusion of CAR^+ T cells (day 0). Tumor burden, as measured by luminescence signal, was monitored by IVIS imaging as shown in **A** and quantified in **B**. **B,** Statistical significance ($P < 0.05$) is shown for comparison with HBSS (*), ddNEG CAR ($), and 0.5×10^6 ddBCMA CAR treatment groups (#). Circulating cells isolated from blood on day 14 after CAR T-cell infusion were analyzed for total GFP^+ (i.e., circulating tumor cells) count (**C**), CAR^+ cell count (**D**), percentage of CAR positive in the $hCD45^+/CD3^+$ population (**E**), and for CD4:CD8 ratio (**F**). **C–F,** All quantification is representative of data gathered from 150 µL of a total volume of 175 µL and are shown as average ± s.e.m. ($n = 4$–5). *, $P < 0.05$; **, $P < 0.01$; ***, $P < 0.001$, for indicated comparisons calculated by one-way ANOVA.

rapid tumor clearance (**Fig. 5A** and **B**; Supplementary Fig. S6 and replicated in Supplementary Fig. S7). Analysis of GFP^+ tumor cells in blood collected 14 days after CAR T-cell transfer confirmed these trends (**Fig. 5C**; Supplementary Figs. S6 and S7D).

CAR^+ T cells (D $domain^+$/human $CD45^+/CD3^+$/mouse $CD45^-/GFP^-$) were detected within all treatment groups that received CAR-T (**Fig. 5D**; Supplementary Fig. S7C). Expansions of human T cells in mice are affected by several factors, including xeno- and allo-reactivity in addition to CAR-mediated proliferation and thus are difficult to interpret from a single timepoint. However, T cells isolated on day 14 from mice receiving the lowest doses of ddBCMA CAR T cells (0.5×10^6 and 0.15×10^6 CAR^+ T cells) showed a moderately enhanced proportion of CAR^+ T cells within the human $CD3^+$ T-cell gate (**Fig. 5E**). CAR^+ T cells from mice receiving 0.5×10^6 and 0.15×10^6 ddBCMA CAR T also had a higher proportion of CD8 T cells than in the other treatment groups (**Fig. 5F**). These observations in the lower treatment groups (which repeated in Supplementary Fig. S7E and S7F) may be due to the slower tumor clearance in these mice, which would provide sustained stimulation of and selection for CAR^+ cells.

The antitumor activity of ddBCMA CAR T cells was not associated with toxicities or inflammation as assessed through postmortem

Table 1. Incidence and severity of nontumor cell histopathologic findings.[a]

Group	1	2	3	4	5	6
CAR	**None**	**ddNEG CAR**	**ddBCMA CAR**	**ddBCMA CAR**	**ddBCMA CAR**	**ddBCMA CAR**
Dose (CAR^+ T cells)	**Hanks' Balanced Salt Solution (HBSS) alone**	**4.5×10^6**	**4.5×10^6**	**1.5×10^6**	**0.5×10^6**	**0.15×10^6**
Number of mice	**4**	**5**	**5**	**5**	**5**	**5**
Bone osteolysis, femur						
Grade 1	0	0	0	0	1	1
Grade 2	2	0	0	0	1	1
Grade 3	2	3	0	0	2	3
Grade 4	0	2	0	0	1	0
Bone osteolysis, skull						
Grade 1	0	2	0	0	0	0
Grade 2	2	0	0	0	1	0
Grade 3	2	2	0	0	3	4
Grade 4	0	1	0	0	0	1
Liver, extramedullary hematopoiesis						
Grade 1	1	4	4	5	5	3
Grade 2	0	1	0	0	0	0
Lung, perivascular CAR T-cell infiltrate						
Grade 1	0	2	3	3	2	0
Grade 2	0	0	0	1	0	0
Oral, abscess						
Grade 1	0	1	0	0	0	0
Grade 2	0	0	0	0	0	0
Grade 3	0	1	0	0	0	0
Salivary gland, inflammation						
Grade 2	0	0	0	1	0	0
Skin abscess, maxillofacial						
Grade 1	0	0	1	0	0	0
Grade 2	0	0	1	1	0	3
Grade 3	0	0	0	2	1	0
Grade 4	0	0	0	1	0	0
Grade 5	0	0	0	1	0	0
Skin, dermis, inflammation						
Grade 1	0	0	0	1	0	0
Spleen, extramedullary hematopoiesis						
Grade 1	0	1	5	4	3	0
Grade 2	2	1	0	1	1	2
Grade 3	1	2	0	0	0	3
Grade 4	1	1	0	0	0	0

Note: Reported values indicate number of animals in each group where the described histopathologic findings were noted.
[a]All other tissues examined not listed in this table were within normal limits.

histopathologic tissue analyses of mice sacrificed either day 15 or 21 (**Table 1**; Supplementary Table S5). The observed histopathologic findings were predominantly attributable to tissue disruption associated with the expanding and infiltrating MM.1S tumor cells observed in several tissues in mice treated with negative controls or low dose (0.15×10^6 and 0.5×10^6) ddBCMA CAR T. Microscopic findings associated with tumor infiltration in bone marrow included osteolytic lesions of the bone and myelophthisis (replacement of normal bone marrow with tumor cells) to varying degrees in all except 4.5×10^6 and 1.5×10^6 ddBCMA CAR T-cell treatment groups. One mouse from the high-dose group was euthanized on day 11 after being found with neurological symptoms (walking in circles). Postmortem necropsy and histopathologic findings in this mouse revealed only perivascular round cell infiltrates in lung and EMH in the spleen, both at 1+, which are unremarkable findings compared with other mice in the study. Mononuclear cell infiltrates were noted around the vasculature of the lungs of mice in all T-cell treatment groups except the lowest dose group. Immunohistochemical stain for human CD3 revealed these cells as well as infiltrates in the liver and spleen were human T cells, but no associated histopathologic changes or tissue damage were noted associated with the human $CD3^+$ T-cell infiltrates (data not shown).

Discussion

The number of clinical trials registered around the world examining CAR-T therapies has exploded over the last few years with estimates as high as more than 600 trials registered in the clinicaltrials.gov registry. Virtually all of these therapies rely on antibody fragments as the CAR antigen–binding domain. Herein, we describe the development of a novel BCMA-targeting CAR T-cell therapy using an engineered D domain in the CAR to specifically recognize BCMA on the surface of myeloma cells. *In vitro* and *in vivo* studies with ddBCMA CAR T cells demonstrate specific cytotoxic activity against myeloma tumors together with the hallmarks of T-cell activation, including degranulation, cytokine release, and CAR-T proliferation.

The experiments detailed in this report demonstrate functional comparability between two CARs both of which bind human BCMA but do so through structurally distinct antigen binding domains. For comparison purposes, both ddBCMA and C11D5.3 scFv-CAR derived from bb2121 (26) were expressed in T cells as fusion proteins comprising a conventional CD8α hinge region fused to the 4-1BB and CD3ζ intracellular signaling domains. Although the antigen-binding domains of ddBCMA CAR and C11D5.3-CAR are structurally distinct, the expression patterns across the various CD4, CD8, and memory T-cell subpopulations are remarkably well conserved as are their functional properties related to *in vitro* potency, cytokine secretion, and kinetics of *in vivo* tumor clearance, perhaps due to their overlapping epitope for binding to BCMA (**Fig. 1B**).

The rationale for developing ddBCMA CAR, as well as other D domain–based CARs, is founded in several inherent limitations in the use of scFv-based CARs, including (i) the molecular mass and nonnative configuration of scFvs that hinder the development of functional multispecific and multivalent CAR constructs; (ii) CARs have been associated with antigen-independent tonic signaling leading to an exhausted T-cell phenotype and compromised function; and (iii) intra- and interpatient scFv CAR expression can be highly variable thereby increasing the likelihood of manufacturing failures and introducing potential toxicities related to variable total cell dosing. The heavy and light chain fragments of scFv have been shown to improperly pair with one another. In the context of conventional CAR constructs expressed on T cells this can lead to oligomerization and tonic signaling (16–18, 33). Likewise, when used in a tandem CAR format, scFv may have an even greater tendency to improperly pair heavy and light chains requiring creative protein engineering solutions to overcome the issue (34). This same phenomenon may also be contributing to highly variable expression of CARs during manufacturing (35).

ddBCMA CAR uses an approximately 8 kDa binding domain obtained from a library of synthetic proteins each sharing a common triple helical structure with 12 randomized amino acid substitutions that define the domain's BCMA-binding site. Replacing a conventional scFv BCMA-binding domain (C11D5.3) with ddBCMA results in higher levels of cell surface CAR expression (**Fig. 1G**) but does not induce tonic signaling (**Figs. 2A** and **3G**) or any coincident loss of function. The underlying mechanism(s) promoting high levels of CAR expression without tonic signaling are not well understood but may be attributable to a D domain's compact size and rapid folding unencumbered by disulfide bond formation or glycosylation (24, 25). The same structural advantages of D domains have been leveraged to produce functional bispecific CARs comprising a CD123-binding D domain fused to a scFv with specificity for CD19 (24). The ability to generate functional multispecific CARs using non-scFv scaffolds like D domains, affords the opportunity to develop multispecific CARs to effectively address tumor relapse caused by antigen loss and a means to treat the intrinsic phenotypic diversity of tumors.

The preclinical analyses reported for ddBCMA are consistent with the high levels of CAR expression and antitumor activity seen among the first 16 patients with multiple myeloma treated with the corresponding clinical product, CART-ddBCMA wherein median drug product CAR^+ expression among $CD3^+$ T cells was 74.5% (min:max 61%–87%) and a 100% ORR were observed (36).

Several recent reports have described three additional alternative BCMA-binding scaffolds that are not based on conventional scFvs. JNJ-4528 (LCAR-B38M) uses two distinct camelid V_H domains (VHH) to generate a biepitopic high-affinity BCMA CAR (37). FHVH33 is a monovalent fully human V_H chain-only BCMA CAR that has shown preclinical function equivalent to a conventional scFv CAR using the C11D5.3 scFv (38). And P-BCMA-101 uses a human fibronectin type III domain to create a high-affinity BCMA CAR (39). Although these CARs and ddBCMA CAR use structurally disparate-binding domains, they have all demonstrated robust preclinical antitumor activity both *in vitro* and *in vivo*. These CARs are, however, readily distinguished on the basis of early clinical response rates with JNJ-4528, FHFV33, and CART-ddBCMA reporting robust ORRs in RRMM of 88% to 91% (37, 40, 41), 90% (42), and 100% (36) respectively. These response rates appear to be somewhat better than the corresponding response rates seen with the first FDA-approved BCMA-CART, idecabtagene vicleucel. In contrast, a substantially lower ORRs of 57% to 75% have been reported for P-BCMA-101 (39). The current preclinical and clinical experiences with these distinct CARs preclude a more thorough understanding of the structural attributes that currently guide the functional characteristics of alternative scaffolds in the treatment of multiple myeloma.

Taken together, the preclinical data reported herein position ddBCMA CAR T as a highly effective, novel therapy with a nonhuman, nonimmunoglobulin–derived BCMA-binding domain. These data provide compelling support for the ongoing clinical

development of CART-ddBCMA for the treatment of RRMM (NCT04155749).

Authors' Disclosures

L.K. Richman reports personal fees from Arcellx during the conduct of the study. No disclosures were reported by the other authors.

Authors' Contributions

J.M. Buonato: Investigation, methodology, writing–original draft, writing–review and editing. **J.P. Edwards:** Investigation, methodology, writing–review and editing. **L. Zaritskaya:** Investigation, methodology. **A.R. Witter:** Investigation, methodology, writing–review and editing. **A. Gupta:** Investigation, methodology. **D.W. LaFleur:** Conceptualization, supervision, writing–review and editing. **D.A. Tice:** Supervision, writing–original draft, writing–review and editing. **L.K. Richman:** Supervision, investigation, methodology. **D.M. Hilbert:** Conceptualization, resources, supervision, writing–original draft.

Acknowledgments

The authors are grateful to Noble Life Sciences (Sykesville, MD) for performing mouse studies, Alizee Pathology (Thurmont, MD) for tissue cross reactivity method development and performance, and Abzena (San Diego, CA) for executing *ex vivo* immunogenicity analysis. We thank Alex Druz and Sumbal Khalid for providing manufactured CAR T cells. We are also grateful to colleagues Jenny Mu, Jeffrey Swers, and Sinnie Ng for technical discussions and guidance. This work was fully supported by Arcellx private funding.

The costs of publication of this article were defrayed in part by the payment of page charges. This article must therefore be hereby marked *advertisement* in accordance with 18 U.S.C. Section 1734 solely to indicate this fact.

Received June 22, 2021; revised December 21, 2021; accepted April 12, 2022; published first June 23, 2022.

References

1. Jacobson CA, Maus MV. C(h)AR-ting a new course in incurable lymphomas: CAR T cells for mantle cell and follicular lymphomas. Blood Adv 2020;4:5858–62.
2. Leick MB, Maus MV, Frigault MJ. Clinical perspective: treatment of aggressive B-cell lymphomas with FDA-approved CAR T-cell therapies. Mol Ther 2021;29:433–41.
3. June CH, Sadelain M. Chimeric antigen receptor therapy. N Engl J Med 2018;379:64–73.
4. Locke FL, Ghobadi A, Jacobson CA, Miklos DB, Lekakis LJ, Oluwole OO, et al. Long-term safety and activity of axicabtagene ciloleucel in refractory large B-cell lymphoma (ZUMA-1): a single-arm, multicentre, phase 1–2 trial. Lancet Oncol 2019;20:31–42.
5. Schuster SJ, Bishop MR, Tam CS, Waller EK, Borchmann P, McGuirk JP, et al. JULIET Investigators. Tisagenlecleucel in adult relapsed or refractory diffuse large B-cell lymphoma. N Engl J Med. 2019;380:45–56.
6. Abramson JS, Palomba ML, Gordon LI, Lunning MA, Wang M, Arnason J, et al. Lisocabtagene maraleucel for patients with relapsed or refractory large B-cell lymphomas (TRANSCEND NHL 001): a multicentre seamless design study. Lancet 2020;396:839–52.
7. Carpenter RO, Evbuomwan MO, Pittaluga S, Rose JJ, Raffeld M, Yang S, et al. B-cell maturation antigen is a promising target for adoptive T-cell therapy of multiple myeloma. Clin Cancer Res 2013;19:2048–60.
8. Tai YT, Anderson KC. Targeting B-cell maturation antigen in multiple myeloma. Immunotherapy 2015;7:1187–99.
9. Tai YT, Anderson KC. B-cell maturation antigen (BCMA)-based immunotherapy for multiple myeloma. Expert Opin Biol Ther 2019;19:1143–56.
10. Brudno JN, Maric I, Hartman SD, Rose JJ, Wang M, Lam N, et al. T cells genetically modified to express an anti–B-cell maturation antigen chimeric antigen receptor cause remissions of poor-prognosis relapsed multiple myeloma. J Clin Oncol 2018;36:2267–80.
11. Cohen AD, Garfall AL, Stadtmauer EA, Melenhorst JJ, Lacey SF, Lancaster E, et al. B-cell maturation antigen-specific CAR T cells are clinically active in multiple myeloma. J Clin Invest 2019;129:2210–21.
12. Raje N, Berdeja J, Lin Y, Siegel D, Jagannath S, Madduri D, et al. Anti-BCMA CAR T-cell therapy bb2121 in relapsed or refractory multiple myeloma. N Engl J Med 2019;380:1726–37.
13. Cohen AD, Garfall AL, Dogan A, Lacey SF, Martin C, Lendvai N, et al. Serial treatment of relapsed/refractory multiple myeloma with different BCMA-targeting therapies. Blood Adv 2019;3:2487–90.
14. Davis LN, Sherbenou DW. Emerging therapeutic strategies to overcome drug resistance in multiple myeloma. Cancers 2021;13:1686.
15. June CH, O'Connor RS, Kawalekar OU, Ghassemi S, Milone MC. CAR T-cell immunotherapy for human cancer. Science 2018;359:1361–65.
16. Long AH, Haso WM, Shern JF, Wanhainen KM, Murgai M, Ingaramo M, et al. 4–1BB costimulation ameliorates T-cell exhaustion induced by tonic signaling of chimeric antigen receptors. Nat Med 2015;21:581–90.
17. Frigault MJ, Lee J, Basil MC, Carpenito C, Motohashi S, Scholler J, et al. Identification of chimeric antigen receptors that mediate constitutive or inducible proliferation of T cells. Cancer Immunol Res 2015;3:356–67.
18. Ajina A, Maher J. Strategies to address chimeric antigen receptor tonic signaling. Mol Cancer Ther 2018;17:1795–815.
19. Siegler E, Li S, Kim YJ, Wang P. Designed Ankyrin repeat proteins as Her2 targeting domains in chimeric antigen receptor-engineered T cells. Hum Gene Ther 2017;28:726–36.
20. Han X, Cinay GE, Zhao Y, Guo Y, Zhang X, Wang P. Adnectin-based design of chimeric antigen receptor for T-cell engineering. Mol Ther 2017;25:2466–76.
21. Zajc CU, Dobersberger M, Schaffner I, Mlynek G, Puhringer D, Salzer B, et al. A conformation-specific ON-switch for controlling CAR T cells with an orally available drug. Proc Natl Acad Sci U S A 2020;117:14926–35.
22. Salzer B, Schueller CM, Zajc CU, Peters T, Schoeber MA, Kovacic B, et al. Engineering AvidCARs for combinatorial antigen recognition and reversible control of CAR function. Nat Commun 2020;11:4166.
23. Simeon R, Chen Z. *In vitro*-engineered non-antibody protein therapeutics. Protein Cell 2018;9:3–14.
24. Qin H, Edwards JP, Zaritskaya L, Gupta A, Mu CJ, Fry TJ, et al. Chimeric antigen receptors incorporating D domains targeting CD123 direct potent mono- and bi-specific antitumor activity of T cells. Mol Ther 2019;27:1262–74.
25. Walsh ST, Cheng H, Bryson JW, Roader H, WF DG. Solution structure and dynamics of a *de novo* designed three-helix bundle protein. Proc Natl Acad Sci U S A 1999;96:5486–91.
26. Kalled SL, Hsu Y, inventors; Anti-BCMA antibodies. World Intellectual Property Organization Patent WO 2010/104949 A2. March 10, 2010.
27. Morgan R, Friedman K, inventors; Bluebird Bio, Inc. BCMA Chimeric Antigen Receptors. WO 2016/094304 A2. June 16, 2016.
28. Amended and Restated Master Collaboration Agreement by and between Bluebird Bio, Inc., and Celgene Corporation and Celgene European Investment Company LLC. June 3, 2015. Accessed May 16, 2022. https://www.sec.gov/files/18-04561-E.pdf.
29. Weinstein JS, Hernandez SG, Craft J. T cells that promote B-cell maturation in systemic autoimmunity. Immunol Rev 2012;247:160–71.
30. Betts MR, Koup RA. Detection of T-cell degranulation: CD107a and b. Methods Cell Biol 2004;75:497–512.
31. Ghermezi M, Li M, Vardanyan S, Harutyunyan NM, Gottlieb J, Berenson A, et al. Serum B-cell maturation antigen: a novel biomarker to predict outcomes for multiple myeloma patients. Haematologica 2017;102:785–95.
32. Good CR, Aznar MA, Kuramitsu S, Samareh P, Agarwal S, Donahue G, et al. An NK-like CAR T-cell transition in CAR T-cell dysfunction. Cell 2004;184:6081–100.
33. Weber EW, Parker KR, Sotillo E, Lynn RC, Anbunathan H, Lattin J, et al. Transient rest restores functionality in exhausted CAR-T cells through epigenetic remodeling. Science 2021;372:eaba1786.
34. Qin H, Ramakrishna S, Nguyen S, Fountaine TJ, Ponduri A, Stetler-Stevenson M, et al. Preclinical development of bivalent chimeric antigen receptors targeting both CD19 and CD22. Mol Ther Oncolytics 2018;11:127–37.

35. Berdeja JG, Lin Y, Raje N, Munshi N, Siegel D, Liedtke M et al. Durable clinical responses in heavily pretreated patients with relapsed/refractory multiple myeloma: updated results from a multicenter Study of bb2121 anti-Bcma CAR T-cell therapy. Blood 2017;130:740.
36. Frigault MJ, Rosenblatt J, Raje NS, et al. Phase 1 study of CART-Ddbcma, a CAR-T therapy utilizing a novel synthetic binding domain for the treatment of subjects with relapsed and/or refractory multiple myeloma. December 13, 2021. Accessed May 16, 2022. https://ash.confex.com/ash/2021/webprogram/Paper150980.html.
37. Xu J, Chen LJ, Yang SS, Sun Y, Wu W, Liu YF, et al. Exploratory trial of a biepitopic CAR T-targeting B cell maturation antigen in relapsed/refractory multiple myeloma. Proc Natl Acad Sci U S A 2019;116:9543–51.
38. Lam N, Trinklein ND, Buelow B, Patterson GH, Ojha N, Kochenderfer JN. Anti-BCMA chimeric antigen receptors with fully human heavy-chain-only antigen recognition domains. Nat Commun 2020;11:283.
39. Costello CL. Phase 1/2 study of the safety and response of P-BCMA-101 CAR-T cells in patients with relapsed/refractory (r/r) multiple myeloma (MM) (PRIME) with novel therapeutic strategies. Blood 2020;136:29.
40. Zhao WH, Liu J, Wang BY, Chen YX, Cao XM, Yang Y, et al. A phase 1, open-label study of LCAR-B38M, a chimeric antigen receptor T-cell therapy directed against B-cell maturation antigen, in patients with relapsed or refractory multiple myeloma. J Hematol Oncol 2018;11:141.
41. Madduri D, Usmani SZ, Jagannath S, Singh I, Zudaire E, Yeh TM, et al. Results from CARTITUDE-1: a Phase 1b/2 study of JNJ-4528, a CAR T-cell therapy directed against b-cell maturation antigen (BCMA), in patients with relapsed and/or refractory multiple myeloma (R/R MM). Blood 2019;134:577.
42. Mikkilineni L, Manasanch EE, Vanasse D, Brudno JN, Mann J, Sherry R, et al. Deep and durable remissions of relapsed multiple myeloma on a first-in-humans clinical trial of t cells expressing an anti–B-cell maturation antigen (BCMA) chimeric antigen receptor (CAR) with a fully-human heavy-chain-only antigen recognition domain. Blood 2020;136:50–51.